

# THE WHITE MARBLE OF THE ARCH OF AUGUSTUS (SUSA, NORTH-WESTERN ITALY): MINERALOGICAL AND PETROGRAPHIC ANALYSIS FOR THE DEFINITION OF ITS ORIGIN\*

A. AGOSTONI

*Department of Earth Sciences, University of Torino, Torino, Italy*

F. BARELLO

*Soprintendenza Archeologia del Piemonte, Piazza S. Giovanni 2, 10122 Torino, Italy*

A. BORGHI†

*Department of Earth Sciences, University of Torino, Torino, Italy*

and R. COMPAGNONI

*Department of Earth Sciences, University of Torino, Torino, Italy*

*The Arch of Augustus in Susa (north-western Italy) was built in 9–8 BC by King Cottius, to celebrate the treaty between the Romans and the Gauls. It is made of white marble, which was considered for a long time to be locally extracted, but no archaeometric studies have been performed up to now. Therefore, a multi-analytical study based on petrographic (optical and scanning electron microscopy), electron microprobe and stable isotope analyses was carried out on the marble from the arch and from reference samples, with the aim of defining the provenance. All the data confirmed that white marble belonging to the metamorphosed carbonate cover of the Dora Maira Massif, known as Foresto marble, was used for the Susa Arch. This choice was probably made for economic reasons, but also due to the relative independence of the ruling family of the Alpes Cottiae, which was obviously interested in promoting a local marble.*

**KEYWORDS:** WHITE MARBLE, PROVENANCE, PETROGRAPHIC ANALYSIS, MINERAL CHEMISTRY, SUSA (NORTH-WESTERN ITALY)

## INTRODUCTION

In the context of the Earth sciences, the description and classification of rocks has always been one of the prerequisites for understanding the genetic and evolutionary process of the Earth's crust. More recent is the recognition of the contribution that the Earth sciences can make to the petrographic study of historical ancient stone materials. During recent decades, the development

\*Received 6 October 2015; accepted 16 March 2016

†Corresponding author: email [alessandro.borghia@unito.it](mailto:alessandro.borghia@unito.it)

© 2016 University of Oxford

of archaeometry has made it possible to highlight how the study of the nature and origin of ornamental stones is predominantly a geological matter, which cannot be solved without a petrographic approach (Lazzarini 2004). In particular, a multi-analytical approach is essential for the identification of monuments and artefacts made of white marble, a stone material most commonly traded in antiquity and, most of all, in the Roman age (Matthews 1997; Gorgoni *et al.* 2002; Polikreti 2007; Borghi *et al.* 2009; Ebert *et al.* 2010).

In this paper a multi-analytical case study is presented that led to the characterization of the white marble used for the building of Arch of Augustus in Susa (north-western Italy), the ancient *Segusio*.

The Susa Arch (Fig. 1 (a)) was built in 9–8 BC by the indigenous King Marcus Iulius Cottius, in order to celebrate an agreement between Romans and local Alpine autonomous tribes, and was built entirely of white marble. It is one of the oldest Roman arches and it was part of a complex building programme for the construction of the new capital of the Alpes Cottiae Province (Barello and Gomez Serito, 2013; Barello 2015). It was placed along the ancient road to Gaul, near the Praetorium, the headquarters of the Roman *praefectus*, in the more elevated urban area. Its illustrated friezes are an exceptional historical testimony of the meeting of two different cultures, with representations of religious ceremonies and administrative procedures that took place immediately after the political agreement (13 BC) between the Roman Empire and the local dynast M. I. Cottius, who obtained, on that occasion, Roman citizenship and the title of Prefect (Letta 1976). The architectural design is characteristic of the Roman architecture of the period (Pensabene 2015) and shows the local effort to provide the new capital with infrastructure and monuments typical of contemporary Roman city planning, such as paved streets, temples, a marketplace (forum) and so on. The position in which it was built (at the starting point of the route for the Montgenevre Pass) and his distinctive architectural structure testify to the symbolic significance attributed to the arch, and also demonstrated that it was built with white marble, a stone material considered quite unusual for that period. Actually, in this early part of the imperial age, marble was still a precious material and its use was full of symbolic implications. It was precisely in the Augustan age that the use of marble became widespread in Roman society, not only in the private *luxuria*, but also in the context of public architecture, both civil and sacred, where its introduction became a norm (Pensabene 2002). Therefore, the determination of the provenance (local or exotic) of the marble employed for the Susa Arch has both significant historical and archaeological implications.

The marble appears light-coloured in a macroscopic observation, with the widespread presence of yellow–ochre patina. It may also be noted that a marble has been employed that is distinguished by different aspects regarding the porosity and the degree of anisotropy. Sacco (1907) studied the origin of the marble of the arch in the early part of the 20th century and suggested the use of Foresto marble (middle Susa Valley). More recently, based on stylistic and geotechnical analysis, Betori *et al.* (2009) confirmed the use of a local marble (Chianocco marble). However, despite its importance in terms of archaeology, the Susa Arch marble has never been studied systematically from an archaeometric perspective. The aim of this study is to better define the provenance of the employed marble using a modern petrographic and geochemical approach.

#### THE GEOLOGICAL SETTING OF THE LOCAL WHITE MARBLE

The ‘Chianocco and Foresto marble’ outcrops along the central portion of the Susa Valley (north-western Italy), which corresponds geologically to the meta-carbonate cover of the Dora Maira Massif (Fig. 1 (b)). The Dora Maira Massif is a unit of continental crust belonging to the Penninic Domain in the Western Alps, which was pervasively deformed and metamorphosed

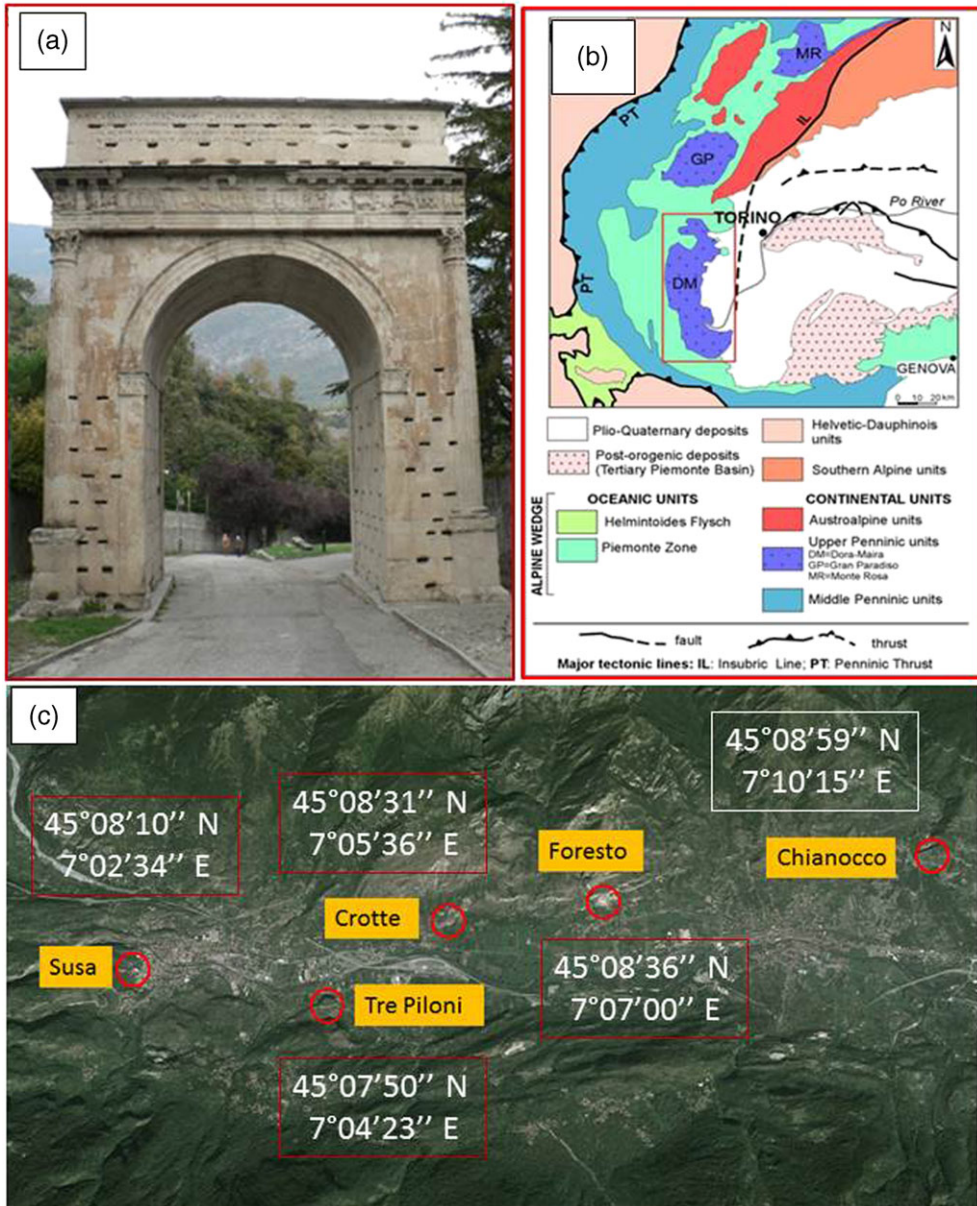


Figure 1 (a) The Arch of Augustus, located at the historic site of Susa (Graian Alps, north-western Italy): it was built along the ancient road to Gaul. (b) A geological sketch map of the Western Alps: the red rectangle points out the Dora Maira Massif. (c) A satellite toponomastic map of the middle Susa Valley (from Google Earth®, 25 July 2015) with the locations of Susa and the four historical quarry sites. [Colour figure can be viewed at [wileyonlinelibrary.com](http://wileyonlinelibrary.com)]

during the Alpine orogeny, which occurred about 50 Ma ago. The Dora Maira Massif is predominantly made up of gneiss and micaschists of Palaeozoic age and rare slices of the original carbonate cover from Triassic to Liassic age, which during Alpine metamorphism became dolomitic marbles and now outcrop along the middle Susa Valley. The Alpine metamorphic cycle resulted in a first

event that developed under eclogitic conditions, during which peak pressure ( $P$ ) and temperature ( $T$ ) conditions were reached, followed by a retrograde metamorphic event that developed under greenschist facies conditions (Gasco *et al.* 2011).

#### SAMPLING AND ANALYTICAL TECHNIQUES

During the study of colour traces commissioned in 2012 by the Superintendence of Archaeological Heritage of Piedmont, a few samples of a small size (a few mm<sup>2</sup>) were collected from different points of the arch. These samples were compared with marble samples collected near Susa, at the localities of Chianocco, Foresto, Crotte and Tre Piloni (Fig. 1 (c)), corresponding to the historical sites of disused quarries.

Petrographic analysis by optical and scanning electron microscopy, together with minero-chemical analysis of the main and accessory minerals by means of an EDS electron microprobe, and finally mass spectroscopy for the determination of stable isotope ratios were carried out. The petrographic analyses were undertaken using a Cambridge S360 scanning electron microscope, connected to an Oxford Instruments Inca Energy 200 EDS equipped with an Oxford SATW Pentafet Si(Li) detector. The analyses were conducted as follows: working distance 25 mm, probe current 200 pA, accelerating potential 20 kV, counting time 60 s. Natural oxides and silicates (Astimex Scientific Limited, Ontario, Canada) were acquired as standards. A cobalt standard was used for instrumental calibration and the relative abundance of the elements was calculated by the instrument software, using the ZAF correction. All the analyses were recalculated using the MINSORT computer program of Petrakakis and Dietrich (1985). The mineral compositions are expressed as atoms per formula unit (apfu). The mineral symbols are those reported by Kretz (1983). The electron microprobe analysis has provided the chemical composition of the main mineral component (calcite and/or dolomite), and the chemical composition of subordinate or accessory minerals that are useful in collecting additional discriminative elements.

A Micro-XRF Eagle III-XPL (Röntgenanalytik Meßtechnik GmbH, Germany) was used for trace element analysis of the calcite and dolomite in the rock samples.

The system includes a Rh X-ray tube, working at a maximum voltage of 50 kV and a maximum current of 1 mA. The X-ray fluorescence is detected by means of a thermoelectrically cooled Si-drift detector, which has an active area of 30 mm<sup>2</sup> and a 5 µm beryllium window. The energy resolution turns out to be lower than 135 eV. Poly-capillary lenses collimate the X-ray microbeam at the sample surface (30 µm). The sample positioning is controlled by a two CCD video cameras, with 10× and 100× magnification, respectively, and optical focusing. The X–Y–Z stage minimum step is 1.5 µm. The instrument can work both in air or in vacuum, and data can be acquired by selecting a single spot, line-scan or element mapping scan mode.

The peak-to-background ratio can be optimized in the energetic range of interest using a set of various primary filters and adjusting the analytical conditions accordingly. The use of filters also minimize the incidence of artefact peaks, which occur in the characteristic X-ray spectra as a result of Bragg diffraction. The selection of proper primary filters is a compromise between optimization of the peak-to-background ratio in the energetic range of interest and the minimization of coherent scattering phenomena. More details of the analytical procedure are reported in Vaggelli and Cossio (2012).

The stable isotope analyses (i.e.,  $\delta^{13}\text{C}$  and  $\delta^{18}\text{O}$ ) have been carried out on calcite and on dolomite for the studied marble types. The protocol reported in McCrea (1950) was followed. In particular, a quantity of 10 mg of powdered calcite or dolomite was reacted with 100% orthophosphoric acid under vacuum conditions. The oxygen and carbon isotopic composition

produced by CO<sub>2</sub> was analysed using a Finningan MAT 250 mass spectrometer. The results are expressed as an isotopic ratio in relation to the PDB standard (Craig 1957), following the convention defined by the International Atomic Energy Agency.

## RESULTS

### *Petrographic analysis*

The petrographic features of the investigated marbles are reported in Table 1 and shown in a series of photomicrographs of representative marble samples (Fig. 2). The Susa Arch samples show a mainly xenoblastic structure, which is characterized by an irregularly shaped aggregate of crystals of calcite and dolomite (Fig. 2 (a)). This feature indicates that the crystallization occurred under syn-kinematic conditions during the development of regional tectonic foliation, which is characteristic of Alpine marbles that outcrop as small and discontinuous lenses interlayered in the crystalline schists of the different tectonic units that make up the Alpine Chain.

The texture of the rock is predominantly anisotropic, with a weak preferred orientation of the mineralogical components, defining the schistosity. The grain size is mainly heteroblastic (HE), although in some samples it is homeoblastic (HO). As for the grain boundary shape (GBS), the arch marble mainly shows irregular crystals marked by boundaries ranging from curved–sutured to embayed. Moreover, single carbonate crystals show polysynthetic twinning and undulate extinction, which reflects the large amount of ductile deformation suffered by the rock under syn-kinematic conditions. The Susa Arch marble shows, only in rare cases, a granoblastic texture, which is characterized by the orderly disposition of carbonate crystals with straight grain boundaries and triple joint contacts (Fig. 2 (b)). This is the typical structure found in marbles crystallized in later static conditions, such as is the case for the marble of the Apuan Alps.

Four representative photomicrographs of the microstructure prevailing for the marbles collected in the historical quarry sites (see Fig. 1 (c)) are shown for comparison. The Foresto (Fig. 2 (c)) and Tre Piloni (Fig. 2 (e)) marbles are characterized by a clear anisotropic texture defined by the preferential dimensional orientation of white mica. The grain size of the carbonate crystals is mainly heteroblastic and the GBS is rather irregular. On the contrary, the Crotte marble (Fig. 2 (d)) is characterized by a typical granoblastic texture with triple joints and crystal boundaries marked by sharp or slightly curved edges. In this case, the lepidoblasts of white mica are not oriented. Finally, the Chianocco marble is characterized by the finer grain size and an isotropic texture, although less regular than that for Crotte marble.

Two important archaeometric parameters have also been measured: the main grain size (MGS) and the average grain size (AGS). The MGS values were collected using a micrometer scale under the optical microscope; the AGS was determined using an image analysis program applied to digital microphotographs acquired at a defined and known magnification. The MGS parameter can provide useful information for the classification of the marble. It is an important diagnostic parameter, strictly related to the maximum temperature reached by the marble during its metamorphic evolution (Moens *et al.* 1988). The diagrams of Figure 3 show that the samples of the Susa Arch have rather homogeneous MGS and AGS values, showing averages ranging from 0.25 to 0.85 mm for the first parameter and from 0.05 to 0.25 mm for the second. If compared to data reported in the literature (e.g., Antonelli and Lazzarini 2015), these two values correspond to fine-grained marbles and reflect conditions of crystallization that occurred at low temperatures; this is consistent with the metamorphic history of the Dora Maira Massif, where

Table 1 The microscopic features of the studied marbles: terminology according to Gorgoni et al. (2002) and mineral abbreviations according to Kretz (1983)

Sample	Grain size	Fabric	Texture	GBS	Accessory minerals												
					Cc	Qtz	Wm	Phl	Chl	Py	Ap	Ep	Tin	Rt	Ox		
ARCH01	Heteroblastic	Xenoblastic	Anisotropic	Straight–curved	x	x	x	x	x	x	x	x	x	x	x	x	x
ARCH03	Heteroblastic	Xenoblastic	Anisotropic	Curved	x	x	x	x	x	x	x	x	x	x	x	x	x
ARCH04	Heteroblastic	Xenoblastic	Anisotropic	Curved	x	x	x	x	x	x	x	x	x	x	x	x	x
ARCH05	Homeoblastic	Granoblastic	Isotropic	Straight–curved	x	x	x	x	x	x	x	x	x	x	x	x	x
ARCH06	Heteroblastic	Xenoblastic	Anisotropic	Straight–curved	x	x	x	x	x	x	x	x	x	x	x	x	x
ARCH08	Heteroblastic	Xenoblastic	Anisotropic	Curved–embayed	x	x	x	x	x	x	x	x	x	x	x	x	x
ARCH09	Heteroblastic	Xenoblastic	Anisotropic	Curved	x	x	x	x	x	x	x	x	x	x	x	x	x
ARCH10	Heteroblastic	Xenoblastic	Anisotropic	Curved–embayed	x	x	x	x	x	x	x	x	x	x	x	x	x
ARCH11	Heteroblastic	Xenoblastic	Anisotropic	Curved	x	x	x	x	x	x	x	x	x	x	x	x	x
ARCH15	Homeoblastic	Granoblastic	Isotropic	Curved	x	x	x	x	x	x	x	x	x	x	x	x	x
ARCH16	Homeoblastic	Granoblastic	Isotropic	Curved	x	x	x	x	x	x	x	x	x	x	x	x	x
ARCH20	Heteroblastic	Granoblastic	Isotropic	Curved–embayed	x	x	x	x	x	x	x	x	x	x	x	x	x
ARCH21	Homeoblastic	Xenoblastic	Anisotropic	Curved–embayed	x	x	x	x	x	x	x	x	x	x	x	x	x
ARCH22	Heteroblastic	Xenoblastic	Anisotropic	Straight–curved	x	x	x	x	x	x	x	x	x	x	x	x	x
ARCH23	Heteroblastic	Xenoblastic	Anisotropic	curved	x	x	x	x	x	x	x	x	x	x	x	x	x

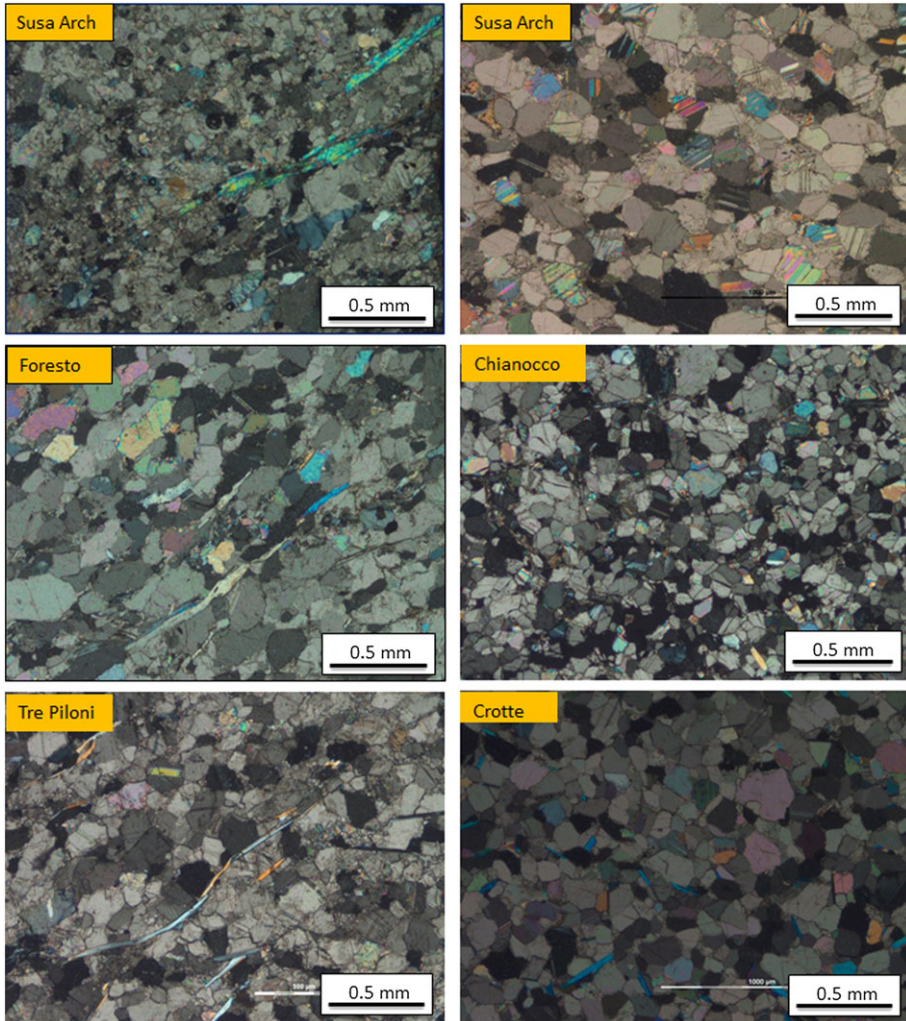


Figure 2 (a,b) Representative microscopic features of the Arch of Augustus marble: (a) microscopic images for the most common variety, characterized by an anisotropic texture defined by the preferential orientation of white mica lamellae (ARCH11); (b) microscopic images for the less common variety, showing a granoblastic and isotropic fabric (ARCH20). (c–f) Representative microscopic features of the marble varieties coming from the four historical quarries located near Susa: the Foresto (c) and Tre Piloni (e) marbles are marked by a syn-kinematic foliated microstructure, while the Chianocco (d) and Crotte (f) marbles show a post-kinematic microstructure defined by a granoblastic fabric and by the occurrence of the typical triple-joints microstructure. [Colour figure can be viewed at [wileyonlinelibrary.com](http://wileyonlinelibrary.com)]

the Alpine metamorphism developed under high-pressure – low-temperature conditions, reaching a peak at around 500 °C (Gasco *et al.* 2011). The comparison with samples collected in the historical quarries of the Susa Valley shows that the Susa Arch marble matches well with the Chianocco, Crotte and Tre Piloni marbles; while the AGS and MGS of the Foresto marble are slightly higher and less homogeneous. A comparison with fine-grained classical Mediterranean marble is also reported in Figure 3 (c). Only the fine-grained group (Carrara, Göktepe,

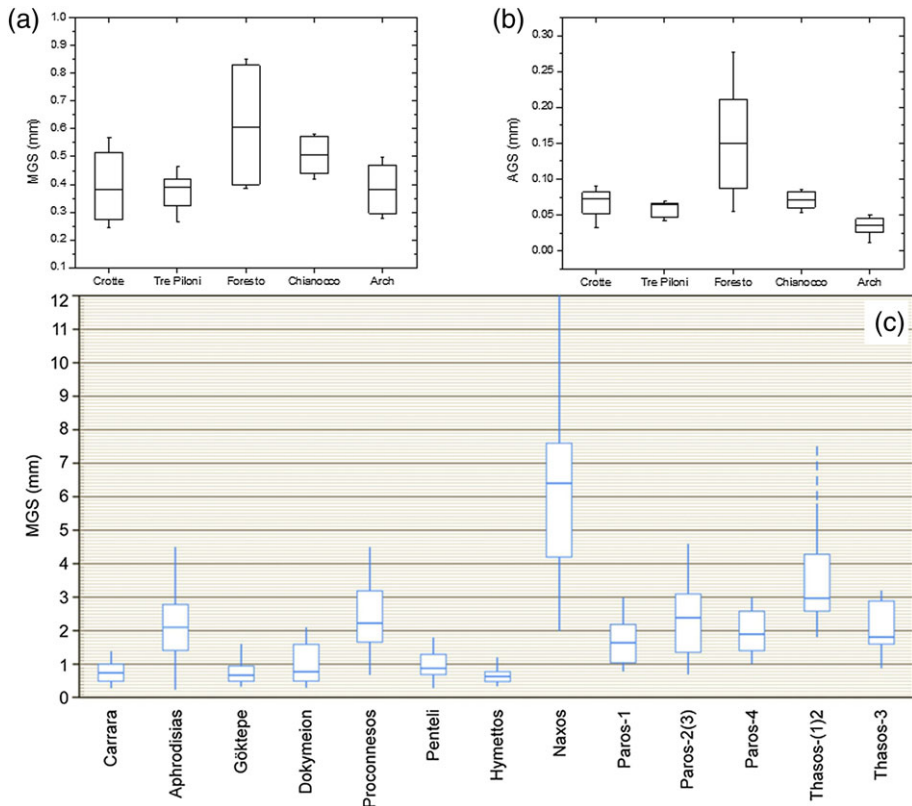


Figure 3 The (a) MGS and (b) AGS parameters for the Arch of Augustus and the four historical Dora Maira marbles. The box charts represent the dispersion of the experimental points: the median and the two percentile values 0.25 and 0.75 are displayed. The bars join the minimum and maximum values. (c) The MGS values for the most common Mediterranean marbles, also reported for a comparison (modified after Antonelli and Lazzarini 2015). [Colour figure can be viewed at [wileyonlinelibrary.com](http://wileyonlinelibrary.com)]

Dokymeion, Penteli and Hymettos) separated by Antonelli and Lazzarini (2015) shows a MGS range compatible with that of the arch marble.

### Mineral chemistry

The examination of representative polished thin sections of the analysed marbles using the SEM–EDS system, employing backscattered electron (BSE) and X-ray signals, allowed us to clearly define the carbonate composition. The brightness signal in the BSE images is sensitive to differences among mean atomic numbers, so the different carbonate phases (i.e., calcite and dolomite) appear as grains at different grey levels; the minerals with higher mean atomic numbers (e.g., calcite) being brighter than those with lighter-forming elements (e.g., dolomite). From a mineralogical point of view, the Susa Arch marble is predominantly composed of dolomite, while calcite is always present, but in lesser amounts (Fig. 4 (a)). Numerous silicatic minerals occur among the accessory minerals. In particular, the most abundant and most significant is the white mica (Fig. 4 (b)), recognized in all samples, which defines the schistosity of the marble. Representative analyses of mica arch samples as well as the micas of the four local quarries are reported in Tables 2 and 3,

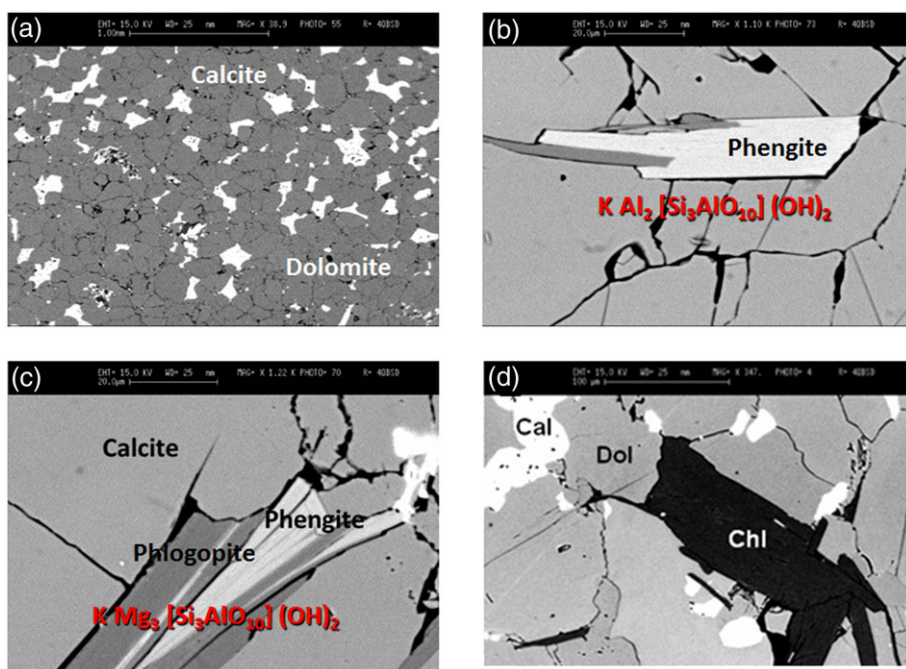


Figure 4 SEM backscattered images for the Arch of Augustus marble: (a) calcite (light) and dolomite (dark) distribution; (b) an oriented phengite crystal, which defines the anisotropy; (c) the phlogopite–phengite association; (d) a rare crystal of chlorite. [Colour figure can be viewed at [wileyonlinelibrary.com](http://wileyonlinelibrary.com)]

respectively. Quartz, iron oxides and pyrite also appear and, occasionally, chlorite, apatite, epidote, sphene and rutile. The presence of rutile, a typical accessory mineral of high-pressure rocks, suggests a local origin for the arch marble, as the various marbles of the Western Alps suffered an eclogitic event that characterized the early metamorphic evolution of the Alpine orogeny. In one sample (ARCH11), phlogopite, the pure Mg end-member of biotite, was also detected (Fig. 4 (c)). Its occurrence in the marbles is relatively rare and therefore can be considered a good marker for the mineralogical characterization of the Susa Arch marble variety. Rare phlogopite crystals were also observed in the samples collected in the Crotte quarry. Representative electron microprobe analyses of phlogopite are reported in Table 4.

The white mica of the Susa Arch samples (ARCH10, ARCH11, ARCH20 and ARCH22), analysed by electron microprobe, shows a phengitic composition and is characterized by a high silicon content, which is, according to the literature, proportional to the pressure (Fig. 5 (a)). In particular, the amount of Si, expressed in the atoms per formula unit (apfu) based on 22 oxygens, varies between 6.93 and 7.24, and is plotted in the field of high-pressure phengite, according to the classification diagram of Capedri *et al.* (2004). The Mg content is between 0.765 and 0.994 apfu, while an Fe content was always absent, consistent with the composition of the carbonatic system. Finally, Ca and Na contents are absent in the site X, in coordination 12, which turns out to be entirely occupied by potassium.

Comparing the composition of the phengitic mica of the Susa Arch marble with the mica samples from the quarries, a partial overlap with those of the Foresto and Tre Piloni marbles can be detected (Fig. 5 (b)). It is worth noting that the micas of the historical quarry samples are much more zoned, showing Si contents between 6.32 and 7.45 apfu. In particular, the micas

Table 2 Representative electron microprobe analyses of white mica from the Susa Arch marble, recalculated on the basis of 22 Ox

Sample Analysis number	ARCH20											ARCH22				
	Ph 1	Ph 2	Ph 3	Ph 4	Ph 5	Ph 6	Ph 7	Ph 8	Ph 9	Ph 10	Ph 11	Ph 12	Ph 13	Ph 14	Ph 15	Ph 16
SiO <sub>2</sub>	54.42	54.22	54.00	54.42	53.28	53.93	54.79	54.09	53.64	53.57	53.69	54.07	54.16	55.00	54.59	54.65
TiO <sub>2</sub>	bdl*	bdl														
Al <sub>2</sub> O <sub>3</sub>	26.19	25.90	24.89	25.83	26.48	24.84	24.92	25.86	27.10	26.40	26.04	24.28	24.76	24.75	24.22	24.76
MgO	4.30	4.38	4.63	4.29	3.99	4.56	4.72	4.47	3.95	3.98	4.15	4.90	4.70	4.96	4.90	4.91
CaO	bdl															
Na <sub>2</sub> O	bdl															
K <sub>2</sub> O	12.11	11.99	12.08	11.96	11.74	11.76	11.88	12.37	12.21	12.25	12.12	11.94	11.88	11.98	12.19	11.77
<b>Total</b>	<b>97.01</b>	<b>96.49</b>	<b>95.61</b>	<b>96.50</b>	<b>95.49</b>	<b>95.09</b>	<b>96.31</b>	<b>96.80</b>	<b>96.91</b>	<b>96.20</b>	<b>95.99</b>	<b>95.19</b>	<b>95.50</b>	<b>96.69</b>	<b>95.90</b>	<b>96.10</b>
Si	7.073	7.083	7.130	7.104	7.027	7.144	7.164	7.064	6.988	7.034	7.060	7.167	7.148	7.169	7.188	7.160
Al IV	0.927	0.917	0.870	0.896	0.973	0.856	0.836	0.936	1.012	0.966	0.940	0.833	0.852	0.831	0.812	0.840
Al VI	3.085	3.071	3.004	3.078	3.143	3.023	3.005	3.045	3.149	3.119	3.094	2.959	3.001	2.970	2.947	2.985
Mg	0.833	0.853	0.911	0.836	0.785	0.900	0.920	0.871	0.768	0.780	0.813	0.969	0.925	0.964	0.962	0.959
Ca	0.000	0.000	0.000	0.000	0.000	0.000	0.000	0.000	0.000	0.000	0.000	0.000	0.000	0.000	0.000	0.000
Na	0.000	0.000	0.000	0.000	0.000	0.000	0.000	0.000	0.000	0.000	0.000	0.000	0.000	0.000	0.000	0.000
K	2.007	1.997	2.035	1.991	1.975	1.988	1.982	2.061	2.029	2.051	2.032	2.019	2.000	1.992	2.048	1.968
Z	8.000	8.000	8.000	8.000	8.000	8.000	8.000	8.000	8.000	8.000	8.000	8.000	8.000	8.000	8.000	8.000
Y	3.917	3.924	3.915	3.914	3.928	3.922	3.925	3.915	3.917	3.898	3.907	3.928	3.925	3.934	3.909	3.944
X	2.007	1.997	2.035	1.991	1.975	1.988	1.982	2.061	2.029	2.051	2.032	2.019	2.000	1.992	2.048	1.968

\*bdl, Below detection limit.

Table 2. (Continued)

Sample	ARCH22						ARCH31						ARCH10					
	Ph 17	Ph 18	Ph 19	Ph 20	Ph 21	Ph 22	Ph 23	Ph 24	Ph 25	Ph 26	Ph 27	Ph 28	Ph 29	Ph 30	Ph 31	Ph 32		
Analysis number																		
SiO <sub>2</sub>	54.94	54.48	54.89	55.20	53.58	54.26	53.84	54.50	54.27	54.36	53.61	54.06	53.58	53.04	54.06	54.15		
TiO <sub>2</sub>	bdl*	bdl																
Al <sub>2</sub> O <sub>3</sub>	24.68	24.77	24.74	23.72	24.56	24.85	26.30	25.30	25.09	24.73	25.44	25.01	27.50	26.75	25.48	26.00		
MgO	4.91	4.80	4.60	5.07	4.53	4.80	4.30	4.59	4.63	4.65	4.41	4.63	3.95	3.97	4.59	4.60		
CaO	bdl																	
Na <sub>2</sub> O	bdl																	
K <sub>2</sub> O	11.97	11.55	12.27	11.51	12.43	12.40	12.36	12.51	12.22	12.27	11.75	11.78	11.67	12.14	11.97	12.04		
<b>Total</b>	<b>96.49</b>	<b>95.61</b>	<b>96.50</b>	<b>95.49</b>	<b>95.09</b>	<b>96.31</b>	<b>96.80</b>	<b>96.91</b>	<b>96.20</b>	<b>95.99</b>	<b>95.19</b>	<b>95.50</b>	<b>96.69</b>	<b>95.90</b>	<b>96.10</b>	<b>96.80</b>		
Si	7.175	7.166	7.179	7.262	7.133	7.126	7.031	7.113	7.124	7.153	7.094	7.132	6.971	6.986	7.094	7.077		
Al IV	0.825	0.834	0.821	0.738	0.867	0.874	0.969	0.887	0.876	0.847	0.906	0.868	1.029	1.014	0.906	0.943		
Al VI	2.973	3.005	2.993	2.939	2.987	2.972	3.079	3.005	3.006	2.988	3.061	3.021	3.187	3.138	3.035	3.051		
Mg	0.956	0.941	0.898	0.994	0.898	0.939	0.837	0.894	0.906	0.912	0.870	0.911	0.765	0.780	0.899	0.893		
Ca	0.000	0.000	0.000	0.000	0.000	0.000	0.000	0.000	0.000	0.000	0.000	0.000	0.000	0.000	0.000	0.000		
Na	0.000	0.000	0.000	0.000	0.000	0.000	0.000	0.000	0.000	0.000	0.000	0.000	0.000	0.000	0.000	0.000		
K	1.994	1.938	2.047	1.931	2.111	2.078	2.059	2.083	2.046	2.060	1.983	1.983	1.937	2.040	2.005	2.002		
Z	8.000	8.000	8.000	8.000	8.000	8.000	8.000	8.000	8.000	8.000	8.000	8.000	8.000	8.000	8.000	8.000		
Y	3.929	3.946	3.891	3.934	3.885	3.911	3.915	3.899	3.912	3.900	3.931	3.932	3.952	3.918	3.933	3.945		
X	1.994	1.938	2.047	1.931	2.111	2.078	2.059	2.083	2.046	2.060	1.983	1.983	1.937	2.040	2.005	2.002		

Table 3 Representative electron microprobe analyses for white mica from historical local Dora Maira quarry marble, recalculated on the basis of 22 Ox

Analysis number	(a) Crotte														(b) Tre Piloni																		
	Ph 1	Ph 2	Ph 3	Ph 4	Ph 5	Ph 6	Ph 7	Ph 8	Ph 9	Ph 10	Ph 11	Ph 12	Ph 13	Ph 14	Ph 15	Ph 16	Ph 1	Ph 2	Ph 3	Ph 4	Ph 5	Ph 6	Ph 7	Ph 8	Ph 9	Ph 10	Ph 11	Ph 12	Ph 13	Ph 14	Ph 15	Ph 16	
SiO <sub>2</sub>	55.83	56.71	54.86	56.66	56.34	56.13	56.93	51.21	54.07	51.79	51.16	53.76	51.37	55.12	53.45	53.58	54.85	51.54	52.60	52.14	49.11	49.45	49.41	52.38	51.58	51.87	56.81	56.46	56.68	59.01	58.98	60.26	
TiO <sub>2</sub>	bdl*	bdl	bdl	bdl*	bdl	bdl																											
Al <sub>2</sub> O <sub>3</sub>	22.75	20.40	22.69	20.56	20.12	19.46	19.91	35.85	33.45	35.41	36.07	31.51	36.22	28.39	29.37	30.39	28.80	29.72	28.49	28.51	32.48	30.75	31.30	28.00	27.27	28.34	26.64	27.10	26.95	22.14	21.90	20.52	
MgO	6.75	7.20	6.41	7.29	7.32	7.50	7.52	1.50	2.41	1.50	1.22	3.18	1.24	4.41	4.92	3.99	4.40	4.04	4.61	4.37	3.11	3.59	3.42	4.97	5.90	4.89	4.85	4.71	4.62	6.48	6.45	6.98	
CaO	bdl	bdl	bdl	bdl	bdl	bdl	bdl	bdl	bdl	bdl	bdl	bdl	bdl	bdl	bdl	bdl	bdl	bdl	bdl														
Na <sub>2</sub> O	bdl	1.37	1.35	1.14	1.31	0.73	1.34	0.30	0.38	0.39	0.28	0.49	0.49	0.46	0.94	0.30	0.47	0.40	0.48	0.51	0.42	0.46	0.35	bdl	bdl	bdl	bdl						
K <sub>2</sub> O	11.67	12.19	11.65	11.99	11.72	12.01	11.93	10.06	8.72	10.16	10.24	10.82	9.83	11.79	11.88	11.66	11.66	11.02	10.71	10.73	10.35	11.11	10.92	10.96	10.65	10.47	11.28	11.39	12.37	12.68	12.24	12.24	
<b>Total</b>	<b>97.01</b>	<b>96.51</b>	<b>95.60</b>	<b>96.50</b>	<b>95.49</b>	<b>95.10</b>	<b>96.30</b>	<b>97.01</b>	<b>96.51</b>	<b>95.60</b>	<b>96.50</b>	<b>95.49</b>	<b>95.10</b>	<b>96.30</b>	<b>96.80</b>	<b>96.90</b>	<b>95.19</b>	<b>96.80</b>	<b>96.90</b>	<b>96.20</b>	<b>95.99</b>	<b>95.19</b>	<b>95.50</b>	<b>96.69</b>	<b>95.90</b>	<b>96.10</b>	<b>96.10</b>	<b>96.10</b>	<b>97.01</b>	<b>97.01</b>	<b>96.51</b>	<b>96.51</b>	
Si	7.252	7.427	7.235	7.411	7.438	7.461	7.461	6.409	6.693	6.474	6.406	6.736	6.414	6.937	6.754	6.749	7.252	7.427	7.235	7.411	7.438	7.461	7.461	6.409	6.693	6.474	6.406	6.736	6.414	6.937	6.754	6.749	
Al IV	0.748	0.573	0.765	0.589	0.562	0.539	0.539	1.591	1.307	1.526	1.594	1.264	1.586	1.063	1.246	1.251	0.748	0.573	0.765	0.589	0.562	0.539	0.539	1.591	1.307	1.526	1.594	1.264	1.586	1.063	1.246	1.251	
Al VI	2.734	2.575	2.762	2.582	2.569	2.509	2.535	3.697	3.572	3.690	3.728	3.390	3.745	3.148	3.128	3.261	2.734	2.575	2.762	2.582	2.569	2.509	2.535	3.697	3.572	3.690	3.728	3.390	3.745	3.148	3.128	3.261	
Mg	1.307	1.405	1.259	1.421	1.442	1.487	1.469	0.280	0.445	0.280	0.228	0.594	0.231	0.827	0.927	0.749	1.307	1.405	1.259	1.421	1.442	1.487	1.469	0.280	0.445	0.280	0.228	0.594	0.231	0.827	0.927	0.749	
Ca	0.000	0.000	0.000	0.000	0.000	0.000	0.000	0.000	0.000	0.000	0.000	0.000	0.000	0.000	0.000	0.000	0.000	0.000	0.000	0.000	0.000	0.000	0.000	0.000	0.000	0.000	0.000	0.000	0.000	0.000	0.000	0.000	
Na	0.000	0.000	0.000	0.000	0.000	0.000	0.000	0.332	0.324	0.276	0.318	0.177	0.324	0.073	0.093	0.095	0.000	0.000	0.000	0.000	0.000	0.000	0.000	0.332	0.324	0.276	0.318	0.177	0.324	0.073	0.093	0.095	
K	1.933	2.036	1.961	2.002	1.974	2.037	1.995	1.606	1.377	1.620	1.636	1.730	1.566	1.893	1.915	1.874	1.933	2.036	1.961	2.002	1.974	2.037	1.995	1.606	1.377	1.620	1.636	1.730	1.566	1.893	1.915	1.874	
Z	8.000	8.000	8.000	8.000	8.000	8.000	8.000	8.000	8.000	8.000	8.000	8.000	8.000	8.000	8.000	8.000	8.000	8.000	8.000	8.000	8.000	8.000	8.000	8.000	8.000	8.000	8.000	8.000	8.000	8.000	8.000	8.000	
Y	4.041	3.981	4.021	4.003	4.010	3.996	4.005	3.977	4.017	3.970	3.956	3.984	3.975	3.975	4.055	4.010	4.041	3.981	4.021	4.003	4.010	3.996	4.005	3.977	4.017	3.970	3.956	3.984	3.975	3.975	4.055	4.010	
X	1.933	2.036	1.961	2.002	1.974	2.037	1.995	1.939	1.701	1.896	1.954	1.907	1.890	1.966	2.008	1.969	1.933	2.036	1.961	2.002	1.974	2.037	1.995	1.939	1.701	1.896	1.954	1.907	1.890	1.966	2.008	1.969	
SiO <sub>2</sub>	54.85	51.54	52.60	52.14	49.11	49.45	49.41	52.38	51.58	51.87	56.81	56.46	56.68	59.01	58.98	60.26	54.85	51.54	52.60	52.14	49.11	49.45	49.41	52.38	51.58	51.87	56.81	56.46	56.68	59.01	58.98	60.26	
TiO <sub>2</sub>	bdl*	bdl	bdl	bdl*	bdl	bdl																											
Al <sub>2</sub> O <sub>3</sub>	28.80	29.72	28.49	28.51	32.48	30.75	31.30	28.00	27.27	28.34	26.64	27.10	26.95	22.14	21.90	20.52	28.80	29.72	28.49	28.51	32.48	30.75	31.30	28.00	27.27	28.34	26.64	27.10	26.95	22.14	21.90	20.52	
MgO	4.40	4.04	4.61	4.37	3.11	3.59	3.42	4.97	5.90	4.89	4.85	4.71	4.62	6.48	6.45	6.98	4.40	4.04	4.61	4.37	3.11	3.59	3.42	4.97	5.90	4.89	4.85	4.71	4.62	6.48	6.45	6.98	
CaO	bdl	bdl	bdl	bdl	bdl	bdl	bdl	bdl	bdl	bdl	bdl	bdl	bdl	bdl	bdl	bdl	bdl	bdl	bdl														
Na <sub>2</sub> O	0.28	0.49	0.49	0.46	0.94	0.30	0.47	0.40	0.48	0.51	0.42	0.46	0.35	bdl	bdl	bdl	0.28	0.49	0.49	0.46	0.94	0.30	0.47	0.40	0.48	0.51	0.42	0.46	0.35	bdl	bdl	bdl	
K <sub>2</sub> O	11.66	11.02	10.71	10.73	10.35	11.11	10.92	10.96	10.65	10.47	11.28	11.28	11.39	12.37	12.68	12.24	11.66	11.02	10.71	10.73	10.35	11.11	10.92	10.96	10.65	10.47	11.28	11.28	11.39	12.37	12.68	12.24	
<b>Total</b>	<b>95.19</b>	<b>96.80</b>	<b>96.90</b>	<b>96.20</b>	<b>95.99</b>	<b>95.19</b>	<b>95.50</b>	<b>96.69</b>	<b>95.90</b>	<b>96.10</b>	<b>95.50</b>	<b>96.69</b>	<b>95.90</b>	<b>96.10</b>	<b>97.01</b>	<b>96.51</b>	<b>95.19</b>	<b>96.80</b>	<b>96.90</b>	<b>96.20</b>	<b>95.99</b>	<b>95.19</b>	<b>95.50</b>	<b>96.69</b>	<b>95.90</b>	<b>96.10</b>	<b>96.10</b>	<b>97.01</b>	<b>97.01</b>	<b>96.51</b>	<b>96.51</b>		
Si	6.900	6.704	6.817	6.808	6.44	6.554	6.523	6.817	6.778	6.780	7.120	7.078	7.105	7.431	7.441	7.575	6.900	6.704	6.817	6.808	6.44	6.554	6.523	6.817	6.778	6.780	7.120	7.078	7.105	7.431	7.441	7.575	

(Continues)

Table 3 (Continued)

Al IV	1.100	1.296	1.183	1.192	1.560	1.446	1.477	1.183	1.222	1.220	0.880	0.922	0.895	0.569	0.559	0.425
Al VI	3.170	3.259	3.169	3.196	3.458	3.357	3.391	3.112	3.001	3.146	3.054	3.082	3.087	2.716	2.697	2.615
Mg	0.825	0.783	0.891	0.850	0.608	0.709	0.673	0.964	1.155	0.953	0.906	0.880	0.863	1.216	1.213	1.308
Ca	0.000	0.000	0.000	0.000	0.000	0.000	0.000	0.000	0.000	0.000	0.000	0.000	0.000	0.000	0.000	0.000
Na	0.068	0.125	0.124	0.117	0.239	0.078	0.120	0.100	0.122	0.129	0.102	0.112	0.085	0.000	0.000	0.000
K	1.871	1.828	1.77	1.787	1.731	1.879	1.838	1.819	1.786	1.747	1.803	1.804	1.822	2.041	2.041	1.963
Z	8.000	8.000	8.000	8.000	8.000	8.000	8.000	8.000	8.000	8.000	8.000	8.000	8.000	8.000	8.000	8.000
Y	3.995	4.042	4.060	4.046	4.066	4.066	4.064	4.076	4.156	4.099	3.960	3.962	3.950	3.933	3.910	3.923
X	1.940	1.952	1.895	1.904	1.970	1.957	1.958	1.919	1.908	1.876	1.905	1.916	1.907	1.987	2.041	1.963
(c) Foresto																
SiO <sub>2</sub>	54.95	54.67	59.02	59.12	57.38	54.20	51.16	51.94	51.21	59.01	58.98	54.07	51.79	51.16	56.89	55.88
TiO <sub>2</sub>	bdl*	bdl														
Al <sub>2</sub> O <sub>3</sub>	28.59	28.59	20.46	20.67	23.73	29.64	33.83	32.30	35.85	22.14	21.90	33.45	35.41	36.07	25.88	26.72
MgO	4.36	4.85	7.89	7.81	6.70	4.54	3.24	3.77	1.50	6.48	6.45	2.41	1.50	1.22	4.90	4.62
CaO	bdl															
Na <sub>2</sub> O	0.33	bdl	bdl	bdl	bdl	0.48	0.98	0.32	1.37	bdl	bdl	1.35	1.14	1.31	bdl	bdl
K <sub>2</sub> O	11.77	11.89	12.63	12.39	12.19	11.15	10.78	11.67	10.06	12.37	12.68	8.72	10.16	10.24	12.34	12.78
<b>Total</b>	<b>96.20</b>	<b>95.99</b>	<b>95.60</b>	<b>96.50</b>	<b>95.49</b>	<b>95.10</b>	<b>96.30</b>	<b>96.80</b>	<b>96.90</b>	<b>96.20</b>	<b>95.99</b>	<b>95.19</b>	<b>95.50</b>	<b>96.69</b>	<b>95.90</b>	<b>96.10</b>
Si	6.917	6.885	7.461	7.461	7.235	6.808	6.44	6.554	6.409	7.431	7.441	6.693	6.474	6.406	7.164	7.064
Al IV	1.083	1.115	0.539	0.539	0.765	1.192	1.56	1.446	1.591	0.569	0.559	1.307	1.526	1.594	0.836	0.936
Al VI	3.159	3.128	2.509	2.535	2.762	3.196	3.458	3.357	3.697	2.716	2.697	3.572	3.690	3.728	3.005	3.045
Mg	0.818	0.911	1.487	1.469	1.259	0.850	0.608	0.709	0.280	1.216	1.213	0.445	0.280	0.228	0.920	0.871
Ca	0.000	0.000	0.000	0.000	0.000	0.000	0.000	0.000	0.000	0.000	0.000	0.000	0.000	0.000	0.000	0.000
Na	0.081	0.100	0.000	0.000	0.000	0.117	0.239	0.078	0.332	0.000	0.000	0.324	0.276	0.318	0.000	0.000
K	1.890	1.910	2.037	1.995	1.961	1.787	1.731	1.879	1.606	1.987	2.041	1.377	1.620	1.636	1.982	2.061
Z	8.000	8.000	8.000	8.000	8.000	8.000	8.000	8.000	8.000	8.000	8.000	8.000	8.000	8.000	8.000	8.000
Y	3.977	4.039	3.956	4.005	4.021	4.046	4.066	4.066	3.977	3.933	3.910	4.017	3.970	3.956	3.925	3.915
X	1.971	1.910	2.037	1.995	1.961	1.904	1.970	1.957	1.939	1.987	2.041	1.701	1.896	1.954	1.982	2.061
(d) Chianocco																
SiO <sub>2</sub>	53.59	54.59	54.31	54.77	54.31	53.23	54.33	52.99	54.23	53.76	54.71	52.67	54.27	54.19	54.25	49.61
TiO <sub>2</sub>	bdl*	bdl														

(Continues)

Table 3 (Continued)

Al <sub>2</sub> O <sub>3</sub>	27.07	24.22	24.61	24.60	24.87	25.99	25.22	26.72	25.56	25.81	25.40	28.53	25.18	25.69	26.07	22.90
MgO	3.95	4.90	4.88	4.91	4.80	4.25	4.58	3.97	4.61	4.56	4.76	4.42	4.91	4.74	4.71	4.30
CaO	Bdl	5.32														
Na <sub>2</sub> O	Bdl															
K <sub>2</sub> O	12.20	12.19	11.70	11.93	12.42	12.22	12.47	12.13	12.01	11.95	12.70	12.01	12.50	12.38	11.80	10.37
<b>Total</b>	<b>96.80</b>	<b>95.92</b>	<b>95.49</b>	<b>96.21</b>	<b>96.40</b>	<b>95.68</b>	<b>96.60</b>	<b>95.81</b>	<b>96.39</b>	<b>96.10</b>	<b>97.61</b>	<b>97.63</b>	<b>96.93</b>	<b>97.05</b>	<b>96.86</b>	<b>92.50</b>
Si	6.988	7.188	7.160	7.175	7.126	7.031	7.113	6.986	7.094	7.057	7.099	6.815	7.090	7.063	7.055	6.889
Al IV	1.012	0.812	0.840	0.825	0.874	0.969	0.887	1.014	0.906	0.943	0.901	1.185	0.910	0.937	0.945	1.111
Al VI	3.149	2.947	2.985	2.973	2.972	3.079	3.005	3.138	3.035	3.051	2.982	3.166	2.966	3.008	3.051	2.637
Mg	0.768	0.962	0.959	0.956	0.939	0.837	0.894	0.780	0.899	0.893	0.921	0.852	0.956	0.921	0.914	0.890
Ca	0.000	0.000	0.000	0.000	0.000	0.000	0.000	0.000	0.000	0.000	0.005	0.000	0.000	0.006	0.004	0.000
Na	0.000	0.000	0.000	0.000	0.000	0.000	0.000	0.000	0.000	0.000	0.000	0.000	0.000	0.000	0.000	0.000
K	2.029	2.048	1.968	1.994	2.078	2.059	2.083	2.040	2.005	2.002	2.102	1.852	1.956	1.921	1.914	1.890
Z	8.000	8.000	8.000	8.000	8.000	8.000	8.000	8.000	8.000	8.000	8.000	8.000	8.000	8.000	8.000	8.000
Y	3.917	3.909	3.944	3.929	3.911	3.915	3.899	3.918	3.933	3.945	3.909	4.018	3.930	3.935	3.968	3.527
X	2.029	2.048	1.968	1.994	2.078	2.059	2.083	2.040	2.005	2.002	2.102	1.983	2.083	2.059	1.958	1.836

<sup>a</sup> bdl, Below detection limit.

Table 4 Representative electron microprobe analyses of phlogopite, recalculated on the basis of 22 Ox

Sample Analysis number	Susa Arch marble, ARCH11					Local quarry marble, Crotte						
	Phl 1	Phl 2	Phl 3	Phl 4	Phl 5	Phl 6	Phl 7	Phl 8	Phl 9	Phl 10	Phl 11	Phl 12
SiO <sub>2</sub>	46.29	46.05	46.73	45.85	45.78	47.12	46.09	45.85	46.72	46.87	45.98	45.34
TiO <sub>2</sub>	bdl*	bdl	bdl	bdl	bdl	bdl	bdl	bdl	bdl	bdl	bdl	bdl
Al <sub>2</sub> O <sub>3</sub>	12.66	12.45	14.59	12.81	12.46	12.06	12.20	12.02	12.15	12.86	12.54	13.32
FeO	bdl	bdl	bdl	bdl	bdl	bdl	bdl	bdl	bdl	bdl	bdl	Bdl
MnO	bdl	bdl	bdl	bdl	bdl	bdl	bdl	bdl	bdl	bdl	bdl	Bdl
MgO	27.42	27.06	24.04	27.12	26.95	27.39	27.92	27.42	27.85	27.26	27.20	27.79
CaO	bdl	bdl	bdl	bdl	bdl	bdl	bdl	bdl	bdl	bdl	bdl	Bdl
Na <sub>2</sub> O	bdl	bdl	bdl	bdl	bdl	bdl	bdl	bdl	bdl	bdl	bdl	Bdl
K <sub>2</sub> O	10.83	11.14	11.14	11.32	11.41	10.83	10.60	10.61	10.27	10.91	10.67	8.67
<b>Total</b>	<b>97.19</b>	<b>96.70</b>	<b>96.50</b>	<b>97.10</b>	<b>96.60</b>	<b>97.40</b>	<b>96.80</b>	<b>95.89</b>	<b>97.00</b>	<b>97.90</b>	<b>96.40</b>	<b>95.11</b>
Si	6.258	6.271	6.339	6.227	6.254	6.348	6.254	6.282	6.306	6.285	6.264	6.189
Al IV	1.742	1.729	1.661	1.773	1.746	1.652	1.746	1.718	1.694	1.715	1.736	1.811
Al VI	0.274	0.270	0.671	0.277	0.260	0.263	0.205	0.222	0.240	0.318	0.277	0.331
Ti	0.000	0.000	0.000	0.000	0.000	0.000	0.000	0.000	0.000	0.000	0.000	0.000
Fe	0.000	0.000	0.000	0.000	0.000	0.000	0.000	0.000	0.000	0.000	0.000	0.000
Mn	0.000	0.000	0.000	0.000	0.000	0.000	0.000	0.000	0.000	0.000	0.000	0.000
Mg	5.526	5.493	4.860	5.491	5.489	5.501	5.648	5.600	5.603	5.448	5.525	5.665
Ca	0.000	0.000	0.000	0.000	0.000	0.000	0.000	0.000	0.000	0.000	0.000	0.000
Na	0.000	0.000	0.000	0.000	0.000	0.000	0.000	0.000	0.000	0.000	0.000	0.000
K	1.868	1.935	1.927	1.962	1.988	1.861	1.835	1.854	1.769	1.865	1.855	1.510

\* bdl, Below detection limit.

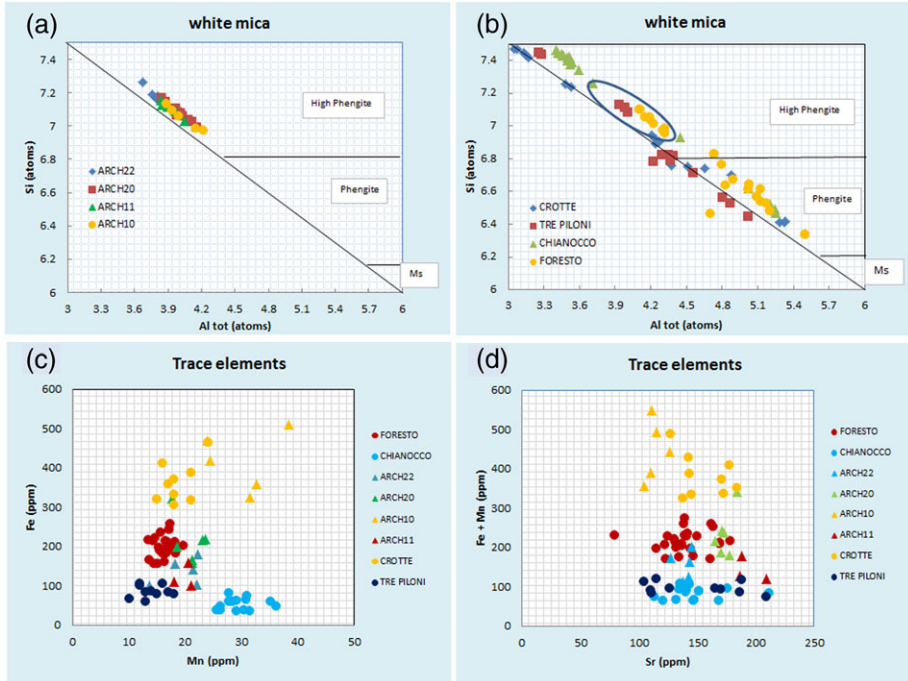


Figure 5 (a,b) The Si–Al<sub>tot</sub> classification diagrams for white mica from the Arch of Augustus and the local quarries, respectively. The ellipse in (b) represents the field in which the phengitic mica of the arch samples is shown to project. The fields of high phengite (High-Phe), phengite (Phe) and muscovite (Ms) are reported according to Capedri et al. (2004). (c,d) The trace element distributions for (c) Fe versus Mn and (d) (Fe + Mn) versus Sr of the investigated marble. [Colour figure can be viewed at [wileyonlinelibrary.com](http://wileyonlinelibrary.com)]

of the Chianocco and Tre Piloni quarries are the ones that are richer in Si. This zoning can be attributed to the effects of partial retrogression of phengite towards muscovite during the second metamorphic event that affected the Dora Maira Massif, which took place in conditions of low pressure.

Chlorite is present in the same marbles where muscovite occurs. The chlorite analysed, both those in the quarry samples and in those of the marble used in the Arch of Augustus (Fig. 4 (d)), was always very homogeneous from a compositional point of view. Its chemical composition is shown in Table 5. In particular, using the classification diagram of Hey (1954), chlorite is projected at the boundary of the clinocllore and pennina fields, being characterized by Si contents ranging between 6.009 and 6.316 apfu, based on 28 oxygens and null values of Fe.

For a better discrimination of Susa Arch marble, the contents of three trace elements (Fe, Mn and Sr) were determined, by using the micro-X-ray fluorescence technique. The results are expressed in parts per million (ppm) and are plotted in Figures 5 (c) and 5 (d). Three (ARCH11, ARCH20 and ARCH22) of the four samples of the Susa Arch are characterized by rather homogeneous values, while sample ARCH10 is characterized by a greater compositional variation. In particular, the Mn content is the lowest and ranges between 14 and 28 ppm, followed by the Sr content, which varies between 105 and 184 ppm. Iron has been an interesting element in this study. Its content is rather homogeneous for samples ARCH11, ARCH20 and ARCH22, varying from 101 to 215 ppm, while sample ARCH10 shows significantly higher values, from 358 to 511 ppm.

Examining the trace element data obtained for the samples from historical quarries, it can be asserted that the trace element contents of the four quarry sites are characterized by narrow

Table 5 Representative electron microprobe analyses of chlorite recalculated on the basis of 28 Ox

Sample	Susa Arch marble											
	ARCH10			ARCH11			ARCH20			ARCH22		
Analysis number	Chl 1	Chl 2	Chl 3	Chl 4	Chl 5	Chl 6	Chl 7	Chl 8	Chl 9	Chl 10	Chl 11	Chl 12
SiO <sub>2</sub>	34.88	34.20	33.92	33.62	33.63	33.23	34.57	34.28	34.51	35.19	33.86	35.09
TiO <sub>2</sub>	bdl*	bdl										
Al <sub>2</sub> O <sub>3</sub>	20.56	21.26	21.27	21.89	21.34	22.21	21.13	21.65	21.19	20.75	21.34	19.98
Cr <sub>2</sub> O <sub>3</sub>	bdl	bdl	bdl	bdl	bdl	bdl	bdl	bdl	bdl	bdl	bdl	bdl
FeO	bdl	bdl	bdl	bdl	bdl	bdl	bdl	bdl	bdl	bdl	bdl	bdl
MnO	bdl	bdl	bdl	bdl	bdl	bdl	bdl	bdl	bdl	bdl	bdl	bdl
MgO	32.56	31.76	32.93	33.00	32.90	32.10	32.78	32.78	32.91	32.99	32.77	33.62
CaO	bdl	bdl	bdl	bdl	bdl	bdl	bdl	bdl	bdl	bdl	bdl	bdl
Na <sub>2</sub> O	bdl	bdl	bdl	bdl	bdl	bdl	bdl	bdl	bdl	bdl	bdl	bdl
K <sub>2</sub> O	bdl	bdl	bdl	bdl	bdl	bdl	bdl	bdl	bdl	bdl	bdl	bdl
<b>Total</b>	<b>88.01</b>	<b>87.23</b>	<b>88.12</b>	<b>88.52</b>	<b>87.87</b>	<b>87.55</b>	<b>88.48</b>	<b>88.71</b>	<b>88.61</b>	<b>88.92</b>	<b>87.98</b>	<b>88.69</b>
Si	6.316	6.247	6.146	6.068	6.113	6.058	6.230	6.165	6.213	6.306	6.144	6.313
Al IV	1.684	1.753	1.854	1.932	1.887	1.942	1.770	1.835	1.787	1.694	1.856	1.687
Al VI	2.702	2.821	2.688	2.725	2.686	2.831	2.718	2.753	2.708	2.688	2.709	2.550
Fe	0.000	0.000	0.000	0.000	0.000	0.000	0.000	0.000	0.000	0.000	0.000	0.000
Mg	8.788	8.645	8.895	8.879	8.915	8.725	8.808	8.788	8.832	8.814	8.865	9.018
Z	8.000	8.000	8.000	8.000	8.000	8.000	8.000	8.000	8.000	8.000	8.000	8.000
Y	11.491	11.466	11.583	11.604	11.601	11.555	11.526	11.541	11.540	11.503	11.573	11.569

\* bdl, Below detection limit.

Table 5 (Continued)

Sample	Local quarry marble											
	CROTTE			CHIANOCCO			FORESTO			TRE PILONI		
Analysis number	Chl 13	Chl 14	Chl 15	Chl 16	Chl 17	Chl 18	Chl 19	Chl 20	Chl 21	Chl 22	Chl 23	Chl 24
SiO <sub>2</sub>	33.94	34.14	34.20	34.29	34.72	34.34	33.30	33.67	34.35	34.00	33.79	33.47
TiO <sub>2</sub>	bdl	bdl	bdl	bdl	bdl	bdl	bdl	bdl	bdl	bdl	bdl	bdl
Al <sub>2</sub> O <sub>3</sub>	20.59	20.52	20.42	20.78	20.63	20.54	21.70	21.02	20.03	21.08	21.00	22.02
Cr <sub>2</sub> O <sub>3</sub>	bdl	bdl	bdl	bdl	bdl	bdl	bdl	bdl	bdl	bdl	bdl	bdl
FeO	0.37	0.38	bdl									
MnO	bdl	bdl	bdl	bdl	bdl	bdl	bdl	bdl	bdl	bdl	bdl	bdl
MgO	33.34	33.25	33.83	33.76	33.73	33.08	33.17	33.34	33.76	33.67	33.29	33.61
CaO	bdl	bdl	bdl	bdl	bdl	bdl	bdl	bdl	bdl	bdl	bdl	bdl
Na <sub>2</sub> O	bdl	bdl	bdl	bdl	bdl	bdl	bdl	bdl	bdl	bdl	bdl	bdl
K <sub>2</sub> O	bdl	bdl	bdl	bdl	bdl	bdl	bdl	bdl	bdl	bdl	bdl	bdl
<b>Total</b>	<b>88.18</b>	<b>88.33</b>	<b>88.46</b>	<b>88.83</b>	<b>89.59</b>	<b>87.96</b>	<b>88.17</b>	<b>88.03</b>	<b>88.13</b>	<b>88.74</b>	<b>88.08</b>	<b>89.10</b>
Si	6.165	6.188	6.181	6.168	6.207	6.231	6.038	6.114	6.228	6.124	6.130	6.009
Al IV	1.835	1.812	1.819	1.832	1.793	1.769	1.962	1.886	1.772	1.876	1.870	1.991
Al VI	2.551	2.572	2.530	2.574	2.553	2.624	2.675	2.613	2.507	2.598	2.620	2.667
Fe	0.063	0.064	0.000	0.000	0.076	0.000	0.000	0.000	0.000	0.000	0.000	0.000
Mg	9.028	8.984	9.114	9.055	8.991	8.949	8.968	9.024	9.125	9.041	9.005	8.994
Z	8.000	8.000	8.000	8.000	8.000	8.000	8.000	8.000	8.000	8.000	8.000	8.000
Y	11.642	11.620	11.644	11.629	11.620	11.573	11.643	11.637	11.632	11.639	11.625	11.662

and well-separated fields. In particular, the Tre Piloni, Foresto and Crotte marbles are distinguished by a progressive increase in the Fe content; while Chianocco is characterized by a low Fe concentration and Mn values in excess of 20 ppm (Fig. 5 (c)). The Sr content, reported in Figure 5 (d), is not discriminating for any of the quarry samples. The Sr concentration ranges between 100 and 220 ppm, with Tre Piloni and Chianocco samples, which turned out to be the most zoned, in respect with the Crotte and Foresto marbles. In Figure 5 (c), the comparison between the arch and quarry samples shows that Fe vs Mn concentration of samples ARCH11, ARCH20 and ARCH22 overlap nicely with the representative fields of the Tre Piloni and Foresto marbles; while sample ARCH10 shows Fe and Mn concentrations comparable with those of the Crotte marble. Finally, none of the arch samples show trace element values compatible with the Chianocco marble. The same considerations apply to the diagram shown in Figure 6 (d).

### C–O stable isotope analysis

The approach based on measurement of the isotopic ratios of carbon and oxygen has produced interesting and promising results ever since its first appearance (Craig and Craig 197). Isotopic data sets were significantly implemented by Moens *et al.* (1988, 1992 and Gorgoni *et al.* (2002), producing excellent reference diagrams for marbles coming from the main quarries that were active in Greek and Roman times.

According to the recent compilations of Lazzarini (2004) and Antonelli and Lazzarini (2015), these diagrams have also been widely used by archaeometrists for other marbles belonging to the Mediterranean basin. However, up to now no isotopic analyses have been reported for the white marbles of the Arch of Augustus at Susa (north-western Italy). For a complete archaeometric characterization of the Susa Arch white marble, C–O stable isotope analyses have been carried out. For comparison, isotopic analyses of local marbles of the Susa Valley have been also reported. Values of  $\delta^{18}\text{O}$  and  $\delta^{13}\text{C}$  have been determined on both calcite and dolomite. The results, referred to the PDB

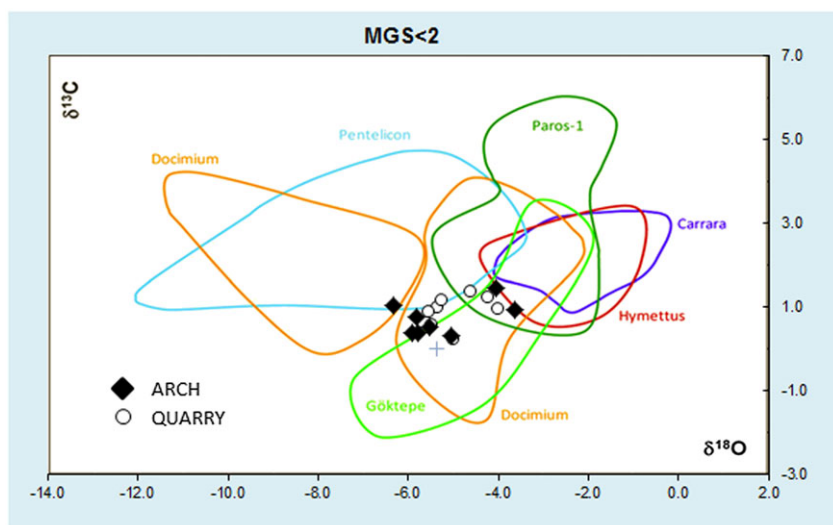


Figure 6 The  $\delta^{13}\text{C}$  versus  $\delta^{18}\text{O}$  diagram for the investigated marbles. The global isotopic reference diagram for the fine-grained marbles (MGS < 2 mm) of the Mediterranean, according to Antonelli and Lazzarini (2015), is also reported for comparison. [Colour figure can be viewed at [wileyonlinelibrary.com](http://wileyonlinelibrary.com)]

standard, are reported in Table 6 and Figure 6. A good correlation between the isotopic data of the arch samples and those of the reference local quarries can be noted. Also, a slightly bimodal distribution may be noted, with the values for the ARCH10 and Crotte marble samples slightly shifted towards higher  $\delta^{18}\text{O}$  values, while most of the data is projected for  $\delta^{18}\text{O}$  values ranging between  $-6.32$  and  $5.04$  and  $\delta^{13}\text{C}$  ranging from  $0.40$  to  $1.04$ . Therefore, even isotopic data suggest that the marble employed for the building of the Arch of Augustus can have a local provenance.

In Figure 6, the characteristic fields for the Mediterranean historical marbles for MGS values  $<2$  mm, according to Antonelli and Lazzarini (2015), were also plotted for comparison. Most of the arch samples fall within the range of *Docimium* marble and, in part, of Goktepe, while the ARCH10 sample, with a higher  $\delta^{18}\text{O}$  ratio, also falls in the field of Paros 1 marble. On the other hand, none of the analysed samples plots in the field of Carrara marble.

#### DISCUSSION AND CONCLUSIONS

In this paper, the white marble used for building the Arch of Augustus at Susa (Cottian Alps, north-western Italy) has been investigated by means of various analytical techniques, such as optical and electron scanning microscopy, the electron microprobe, micro-fluorescence and isotopic analysis, in order to determine its provenance, which can yield some important archaeological implications. The time at which the Susa Arch was built (9 BC) matches with the period when the ancient Susa (*Segusio*) became the political and administrative centre of the Alpine region just conquered by Romans. In this context, the search for good-quality stone materials for monumental apparatus became a primary necessity, which could be achieved by the opening of new marble quarries on the northern side of the middle Susa Valley. This assumption is in agreement with the evaluated archaeometric data, which show a good correlation between the arch samples and those from the local historical quarries, which can be geologically attributed to the carbonate cover of the Dora Maira Massif.

In particular, it can be supposed that the blocks for the Susa Arch originate from the quarry sites of Tre Piloni and Foresto for samples ARCH11, ARCH20 and ARCH22, which show a good fit relative to the microstructural, AGS, isotopic and trace element data. Sample ARCH10, on the other hand, shows a good correlation with Crotte marble (isotropic texture, high concentration of iron, isotopic data). Finally, the analytical data from the marble of the Chianocco quarry turned out to be more different from the samples of the Susa Arch. This could be due to the fact that the Chianocco quarry is further from Susa than the other quarries and, consequently, was used less for the building of the arch.

Table 6 The  $\delta^{13}\text{C}$  and  $\delta^{18}\text{O}$  values of the calcite and dolomite from the Susa Arch and quarry marbles: the  $\delta^{13}\text{C}$  and  $\delta^{18}\text{O}$  data are expressed relative to the PDB standard (Craig 1957); the analytical protocol is according to McCrea (1950)

	$\delta^{13}\text{C}$ , calcite	$\delta^{18}\text{O}$ , calcite	$\delta^{13}\text{C}$ , dolomite	$\delta^{18}\text{O}$ , dolomite
ARCH10	0.95	-3.64	1.47	-4.04
ARCH11	0.40	-5.92	0.52	-5.53
ARCH20	0.78	-5.83	0.31	-5.04
ARCH22	1.04	-6.32	0.40	-5.80
Crotte	1.24	-4.25	0.97	-4.02
Chianocco	1.39	-4.63	1.19	-5.27
Foresto	0.92	-5.55	0.25	-5.01
Tre Piloni	1.01	-5.37	0.59	-5.51

The data therefore suggest the use of local marble rather than the most precious marbles from more distant areas, such as the marble of the Apuan Alps, or even the Greek marbles.

This matter opens up more general considerations. As is known from the literature, in the early years of the Roman Empire, the importation of precious marbles coming from well-known historic sites such as those of Ancient Greece was still rather limited (Pensabene 2002). On the other hand, in that period the use of Luni marble, extracted in the vicinity of the Apuan Alps, became more widespread. However, the data reported in this paper (mainly the anisotropic texture, the occurrence of abundant phengitic mica, the mainly dolomitic composition and the isotopic data) allow us to rule out an Apuan origin with a good degree of certainty. The isotope data suggest, instead, a similarity with Asian marbles, such as the *Docimium* and Göpstepe types, but these marbles were diffused later in the Roman Empire, from the end of the first century AD (Pensabene 2002) and therefore should be excluded from our assumptions of the provenience. The hypothesis of a local origin, therefore, remains the most likely.

With regard to the choice of local stones, it can be supposed that decisions were made for economic reasons, but also due to the relative independence of the ruling family of the Alpes Cottiae, who were obviously interested in promoting a local marble (Pensabene 2005). On the other hand, the use of this local marble was extended for architectural elements not only at *Segusio*, but also in contemporary public and private buildings in the Transpadana region (Betori *et al.* 2009), such as the Almese Villa (Susa Valley) colonnades and the so-called Palatine Gate and the *porticus* of the Roman Theatre in the Roman colony of *Augusta Taurinorum* (present-day Turin), which was founded in around 20 BC, and was for a long time a satellite to the neighbouring small kingdom.

#### ACKNOWLEDGEMENTS

This work was financially supported by the Ministero dell'Università e della Ricerca Scientifica e Tecnologica (MURST) and by the Accademia delle Scienze di Torino. The Segusium (Society for Research and Studies of the Susa Valley) is thanked for its support.

#### REFERENCES

- Antonelli, F., and Lazzarini, L., 2015, An updated petrographic and isotopic reference database for white marbles used in antiquity, *Rendiconti Lincei—Scienze Fisiche e Naturali*, **26**(4), 339–413.
- Barello, F., 2015, Susa augustea, in *L'Arco di Susa e i monumenti della propaganda imperiale in età augustea, Proceedings, Susa, 12 April 2014*, 161–78, Ministero dei beni e delle attività culturali e del turismo, Roma.
- Barello, F., and Gomez Serito, M., 2013, Marmi valsusini per l'edificazione della capitale delle Alpi Cozie: nuovi dati dai recenti scavi, *Bulletin d'études Préhistoriques et Archeologiques Alpines*, **24**, 89–124.
- Betori, A., Gomez Serito, M., and Pensabene, P., 2009, Investigation of marbles and stones used in Augustean monuments of Western Alpine provinces (Italy), in *ASMOSIA VII: proceedings of the 7th International Conference of Association for the Study of Marble and Other Stones in Antiquity, Thassos, 15–20 September 2003* (ed. Y. Maniatis), 89–102, École française d'Athènes, Athens.
- Borghi, A., Fiora, L., Marcon, C., and Vaggelli, G., 2009, The Piedmont white marbles used in antiquity: an archaeometric distinction inferred by a mineralogical-petrographic and C–O stable isotope study, *Archaeometry*, **51**, 913–31.
- Capedri, S., Venturelli, G., and Photiades, A., 2004, Accessory minerals and  $\delta^{18}\text{O}$  and  $\delta^{13}\text{C}$  of marbles from the Mediterranean area, *Journal of Cultural Heritage*, **5**, 27–47.
- Craig, H., 1957, Isotopic standards for carbon and oxygen and correction factor for mass-spectrometric analysis of carbon dioxide, *Geochimica et Cosmochimica Acta*, **12**, 133–49.
- Ebert, A., Gnos, E., Ramseyer, K., Spandler, C., Fleitmann, D., Bitzios, D., and Decrouez, D., 2010, Provenience of marbles from Naxos based on microstructural and geochemical characterization, *Archaeometry*, **52**, 209–28.
- Gasco, I., Gattiglio, M., and Borghi, A., 2011, New insight on the lithostratigraphic setting and on tectono-metamorphic evolution of the Dora Maira vs Piedmont Zone boundary (middle Susa Valley), *Journal of Earth Sciences*, **100**, 1065–85.

- Gorgoni, C., Lazzarini, L., Pallante, P., and Turi, B., 2002, An updated and detailed minero-petrographic and C–O stable isotopic reference database for the main Mediterranean marbles used in antiquity, in *ASMOSIA 5: interdisciplinary studies on ancient stone: proceedings of the fifth international conference of the Association for the Study of Marble and Other Stones in Antiquity, Museum of Fine Arts, Boston, 1998* (eds. J. J. Herrmann, N. Herz, and R. Newman), 115–31, Archetype, London.
- Hey, M. H., 1954, A new review of chlorites, *Mineralogical Magazine*, **30**, 277–92.
- Kretz, R., 1983, Symbols for rock forming minerals, *American Mineralogist*, **68**, 277–9.
- Lazzarini, L., 2004, Archaeometric aspects of white and coloured marbles used in antiquity: the state of the art, *Periodico di Mineralogia*, **73**, 113–25.
- Letta, C., 1976, La dinastia dei Cozii e la romanizzazione delle Alpi Occidentali, *Athenaeum, Studi periodici di letteratura e storia dell'antichità*, **LIV**(1–2), 37–76.
- McCrea, J., 1950, On the isotopic chemistry of carbonates and a paleotemperature scale, *Journal of Chemical Physics*, **18**, 849–57.
- Matthews, K. J., 1997, The establishment of a data base of neutron activation analyses of white marble, *Archaeometry*, **39**, 321–32.
- Moens, L., De Paepe, P., and Waelkens, M., 1992, Multidisciplinary research and cooperation: keys to a successful provenance determination of white marble, in *Ancient stones: quarrying, trade and provenance* (eds. M. Waelkens, N. Herz, and L. Moens), 247–54, Acta Archaeologica Lovaniensia Monographie 4, University Press, Leuven.
- Moens, L., Roos, P., De Rudder, J., Hoste, J., De Paepe, P., Van Hende, J., Marechal, R., and Waelkens, M., 1988, White marble from Italy and Turkey: an archaeometric study based on minor and trace-element analysis and petrography, *Journal of Radioanalytical and Nuclear Chemistry*, **123**, 333–48.
- Pensabene, P., 2002, Il fenomeno del marmo nel mondo romano, in *I marmi colorati della Roma Imperiale* (eds. P. Pensabene and L. Lazzarini), 3–68, Marsilio editore, Venezia.
- Pensabene, P., 2005, Monumenti augustei delle province alpine occidentali: cultura architettonica, materiali e committenza, in *Studi di archeologia in memoria di Liliana Mercado* (ed. M. Sapelli Ragni), 211–29, Soprintendenza per i beni archeologici del Piemonte e del Museo antichità egizie, Torino.
- Pensabene, P., 2015, Arco di Susa: forme della decorazione architettonica, in *L'Arco di Susa e i monumenti della propaganda imperiale in età augustea, Proceedings, Susa, 12 April 2014*, 75–100, Ministero dei beni e delle attività culturali e del turismo, Roma.
- Petrakakis, K., and Dietrich, H., 1985, MINSORT: a program for the processing and archivation of microprobe analyses of silicate and oxide minerals, *Neues Jahrbuch für Mineralogie—Monatshefte*, **8**, 379–84.
- Polikreti, K., 2007, Detection of ancient marble forgery: techniques and limitations, *Archaeometry*, **49**, 603–19.
- Sacco, F., 1907, Geologia applicata della città di Torino, *Giornale di geologia pratica*, **5**, 121–62.
- Vaggelli, G., and Cossio, R., 2012,  $\mu$ -XRF analysis of glasses: a non-destructive utility for cultural heritage applications, *Analyst*, **137**, 662–7.